Studies in Engineering and Exact Sciences
ISSN: 2764-0981

Preparation and characterization of ultrafiltration membranes derived from recycled Polyethylene terephthalate (PET) bottles

Preparação e caracterização de membranas de ultrafiltração derivadas de garrafas de Politereftalato de etileno (PET) recicladas

DOI: 10.54021/seesv5n1-009

Recebimento dos originais: 28/12/2023
Aceitação para publicação: 29/01/2024

Mohammed Amin Chemrak
PhD in Chemical Engineering
Institution: Faculty of Science and Technology, University of Tissemsilt
Address: BP 38004 Tissemsilt, Algéria
E-mail: ma.chemrak@univ-tissemsilt.dz

Abdelkader Chougui
PhD in Chemical Engineering
Institution: IBN Khaldoun University of Tiaret
Address: BP 14000 Tiaret, Algéria
E-mail: abdelkader.chougui@univ-tiaret.dz

Mustapha Hafani
PhD in Chemical Engineering
Institution: University of Mostaganem
Address: BP 188 Mostaganem, Algéria
E-mail: hafanim01@gmail.com

Sara Chourouk Benali
Master in Chemical Engineering
Institution: University of Mostaganem
Address: BP 188 Mostaganem, Algéria
E-mail: benalisc01@gmail.com

Djellal Adda Benattia
Master in Chemical Engineering
Institution: University of Mostaganem
Address: BP 188 Mostaganem, Algéria
E-mail: ben95attia@gmail.com

M'hammed Djennad
Doctor in Chemical Engineering
Institution: University of Mostaganem
Address: BP 188 Mostaganem, Algéria
E-mail: djennadm@yahoo.fr

ABSTRACT

The pressing need for sustainable practices and eco-friendly materials in the face of escalating environmental concerns has led to exploring the transformation of discarded polyethylene terephthalate (PET) bottles into functional ultrafiltration membranes. This research prepares and characterizes ultrafiltration membranes derived from PET bottle waste. The study involves collecting PET waste material and fabrication processes to develop asymmetric flat sheet membranes blended with varying proportions of hydrophilic polyethylene glycol (PEG) using phase inversion techniques. Rigorous characterization employing SEM, EDS analysis, and water vapor permeability (WVP) assessments examine these membranes' structural, morphological, and performance attributes. The surface analysis elucidates a notable correlation between increased PEG content and larger pore sizes, consistent with prior studies involving PEG in membrane modifications. Additionally, incorporating PEG in the casting solution elevates water vapor permeability. Ultrafiltration experiments reveal differing rejection rates, with membrane M2 exhibiting enhanced anti-fouling properties despite reduced flux compared to M3 and M4. This research lays the groundwork for repurposing PET waste into selective membrane materials, emphasizing optimization strategies to enhance membrane quality and performance for diverse operational settings.

Keywords: waste plastic bottle, ultrafiltration membranes, Polyethylene terephthalate (PET), polyethylene glycol (PEG).

RESUMO

A necessidade premente de práticas sustentáveis e materiais ecologicamente corretos em face das crescentes preocupações ambientais levou à exploração da transformação de garrafas de politereftalato de etileno (PET) descartadas em membranas de ultrafiltração funcionais. Esta pesquisa trata da preparação e caracterização de membranas de ultrafiltração derivadas de resíduos de garrafas PET. O estudo envolve a coleta de resíduos de PET e processos de fabricação para desenvolver membranas de folha plana assimétricas misturadas com proporções variáveis de polietilenoglicol (PEG) hidrofílico usando técnicas de inversão de fase. Uma caracterização rigorosa empregando SEM, análise EDS e avaliações de permeabilidade ao vapor de água (WVP) examina os atributos estruturais, morfológicos e de desempenho dessas membranas. A análise da superfície elucida uma correlação notável entre o aumento do conteúdo de PEG e tamanhos maiores de poros, consistente com estudos anteriores envolvendo PEG em modificações de membrana. Além disso, a incorporação de PEG na solução de fundição aumenta a permeabilidade ao vapor de água. Os experimentos de ultrafiltração revelam diferentes taxas de rejeição, com a membrana M2 exibindo propriedades antiincrustantes aprimoradas, apesar do fluxo reduzido em comparação com M3 e M4. Esta pesquisa estabelece as bases para o reaproveitamento de resíduos de PET em materiais de membrana seletiva, enfatizando as estratégias de otimização para melhorar a qualidade e o desempenho da membrana para diversas configurações operacionais.

Palavras-chave: resíduos de garrafas plásticas, membranas de ultrafiltração, Politereftalato de etileno (PET), polietileno glicol (PEG).

1 INTRODUCTION

Amidst a time characterized by growing environmental worries and the urgent need for sustainable solutions, utilizing waste materials to create practical products has become a crucial pathway for ecological preservation and technical progress. Within this framework, the conversion of discarded polyethylene terephthalate (PET) bottles into ultrafiltration membranes presents a promising advancement, providing a dual advantage of waste disposal and the creation of valuable, environmentally friendly materials (JAREONSRI; NAWALERTPANYA; JANTAPORN, 2023; KIRSHANOV et al., 2022; PULIDO et al., 2019). This study article thoroughly investigates the process and analysis of ultrafiltration membranes obtained from discarded PET bottles. Polyethylene terephthalate (PET), a commonly utilized polymer in packaging materials, represents a significant proportion of the world's plastic trash, presenting considerable difficulties in disposal and recycling. Using the intrinsic characteristics of PET to create membranes for ultrafiltration offers a promising chance to reduce environmental impacts and meet urgent requirements in separation technologies (BEGHETTO et al., 2021; KIBRIA et al., 2023; RAJ et al., 2023). Previous studies have shown limitations in the mechanical strength and hydrophilicity of PET membranes derived from waste plastic bottles (MULYATI et al., 2018; RAJESH; MURTHY, 2014). To address these shortcomings, additional modification is needed to improve its properties, such as composite formation by combining PET and other polymeric materials. Considering the efficacy of organic additives, polyethylene glycol (PEG) emerges as a promising candidate due to its multifaceted impact on membrane characteristics, including pore formation, improved hydrophilicity, resistance to fouling, and enhancement of water vapor permeability (WVP) (GEBRU; DAS, 2017; LIN et al., 2007; MA et al., 2012). This study thoroughly examines the recycling process of PET polymer obtained from discarded plastic bottles to create specific membrane materials. The synthesis of asymmetric flat sheet membranes made of hydrophobic PET polymer combined with different quantities of hydrophilic material has been achieved skillfully using phase inversion generated by dry and immersion precipitation procedures. The main objective is to assess the performance of these PET membranes, with a particular emphasis on investigating how the inclusion of hydrophilic material

affects both selectivity and permeability for water vapor applications. The synthesis involves intricate methodologies to convert PET bottle waste into functional ultrafiltration membranes, employing diverse formulation techniques, additives, and fabrication methods. Systematic characterization utilizing analytical tools rigorously assesses these membranes' structural, morphological, and performance aspects, encompassing pore size distribution, surface morphology, mechanical properties, and filtration efficiency. This meticulous analysis aims to establish the feasibility and effectiveness of these recycled PET-based membranes for ultrafiltration applications. Moreover, this study delves into optimization strategies, exploring the impact of various variables such as additives, blending techniques, and processing conditions. By systematically investigating these factors, the research endeavors to enhance membrane quality, permeability, selectivity, and durability, aiming to broaden the applicability and performance of these membranes across diverse operational settings.

2 MATERIALS AND METHODS

2.1 MATERIALS

In this study, the poly (ethylene terephthalate) (PET) utilized was sourced from waste plastic bottles and underwent a purification process through re-precipitation. PET, explicitly derived from recycled plastic bottles, formed the foundational material for membrane synthesis. The PEG (Polyethylene glycol) with an average Mn 6,000 was procured from Merck and served as an essential additive in the membrane fabrication process. Additionally, DCM (Dichloromethane) obtained from Merck was employed as the primary solvent for membrane preparation. Distilled water, utilized as a non-solvent solution, was crucial in the phase inversion procedure. The synthesis of TCA (Trichloroacetic acid) solution, a membrane solvent, involved dissolving TCA crystal powder into DCM, the proportion 2:3 of TCA: DCM based on a previous study we conducted (HAFANI et al., 2021), sourced from EDEN LABO, SARL, Algeria, to facilitate the membrane production process. Each constituent material and solvent utilized in this study was meticulously selected and prepared to ensure precision and reproducibility in membrane synthesis.

2.2 CASTING SOLUTION PREPARATION

Initially, plastic bottles were separated and then sliced into small fragments measuring 5x5 mm². These fragments were subsequently cleaned and washed with distilled water and dried at the ambient temperature of the laboratory for 2 hours. Later, the dehydrated PET flakes were immersed in a solvent mixture of TCA (trichloroacetic acid) and DCM (dichloromethane) at room temperature while constantly agitated with a magnetic bar. Polyethylene glycol (PEG) was dissolved individually in a TCA: DCM solvent under identical conditions. Once the homogenous solutions were acquired, they were combined and stirred for one hour. The homogenous solution was allowed to stand at ambient temperature for approximately 12 hours to eliminate any trapped air bubbles. The casting solutions' compositions are enumerated in Table 1.

Table 1 – The formulation of the membrane casting solution

Membrane	**Polymer (g)**		**Solvent (ml)**
	PET	**PEG**	**TCA: DCM**
M1	10	0	20
M2	9	1	20
M3	8	2	20
M4	7	3	20

Source: Authors.

2.3 PET MEMBRANE FABRICATION

The recently created casting solution was promptly cast onto a pristine glass plate using a glass casting rod while keeping a gap distance of 100 µm. After applying the coating, the solution was left uncovered at room temperature for 5 minutes. Then, it was immersed in a distilled water bath at room temperature. This process lasted at least 24 hours to help remove solvent and water-soluble polymer components. Afterward, the created membranes were dried, and their thickness was measured using a certified digital thickness equipment called the INSIZE series 3109. This device has a range of 0-25 mm and a resolution of 0.001 mm. Before their use, the membranes underwent visual inspection to verify the absence of any faulty spots.

2.4 MEMBRANE CHARACTERIZATION

Examining membrane morphology encompassed surface and cross-sectional features through scanning electron microscopy (SEM) techniques. The FEI Quanta 650 SEM was employed for cross-sectional analysis to elucidate the structural aspects of the synthesized membranes. The examination primarily focused on pore diameter and distribution on the surface, particularly within the porous sublayer, considering the dense and selective layer as non-porous. SEM images exclusively captured the surface of the porous sublayer. Image analysis was conducted using ImageJ software to scrutinize pore size and distribution on the sublayer surface. The surface elemental composition was also determined via energy-dispersive X-ray spectrometry (EDS) analysis using the Bruker QUNATX EDS XFlash® 6|10 integrated into the FEI Quanta 650 SEM setup. This comprehensive analysis aimed to provide insights into synthesized membranes' morphological characteristics and elemental makeup.

2.5 EVALUATION OF PERMEATION AND SEPARATION PERFORMANCE

The water vapor permeability (WVP) of the PET membranes was evaluated using the methods specified in the ASTM E 96 standard (C16.33 COMMITTEE, 2013). Structures with membranes that ranged in thickness from 60 to 130 μm were formed like discs and resembled the cup's opening. An effective area of 30.19 cm^2 was achieved by allowing the ledges to form a seal on the membranes, which added 5 mm. The membranes were carefully placed along the cup's borders and then sealed with a silicone gasket. The cup adheres to standard specifications and was placed inside a custom-made furnace. A temperature controller consistently maintained the temperature inside the stove at an average of 37-39 degrees Celsius. To keep the humidity stable, the furnace door was kept open throughout the experiments, ensuring it remained within the range of 30%. At regular intervals of 2-3 hours, the dish was systematically removed and subjected to weighing to ascertain the temporal loss of water. Subsequently, this data served as the basis for calculating the WVP within the stable zone. To ensure the consistency and reliability of the results, a minimum of three samples were tested under each condition, with the calculation WVP from the formula (C16.33 COMMITTEE, 2013):

$$WVP = \frac{G.l}{S\,(R1-R2).t.A} \quad (1)$$

Where:

G is the weight change, [g], *l* is the thickness of the membrane specimen, [μm], S is the vapor pressure at test temperature (37 °C), [Pa], R1 is the relative humidity in the dish (nominally 100% for the water), [%], R2 is the relative humidity inside the oven, [%], t is the time, [s], and A is testing area, [m^2].

The ultrafiltration capacity of the membranes was assessed by specific experiments conducted using the equipment illustrated in Figure 1. The membrane was situated within a membrane module featuring a membrane area of 30.19 cm^2. The testing employed a feed solution, including a Bovine Serum Albumin solution with a concentration of 1000 ppm, which served as the solute model. The operational parameters maintained a transmembrane pressure of 1 bar at around 25 °C. The ultrafiltration procedure was carried out for 2 hours, during which the permeate was gathered and quantified at 5-minute intervals. The membrane rejection (R) was obtained by quantifying the concentrations of BSA in the permeate (CP) and the feed solution (CF) using the following equation:

$$R = \left(1 - \frac{C_P}{C_F}\right) \times 100 \quad (2)$$

Where:

C_P is solute concentration in the permeate stream, [ppm], and CF is in the feed stream, [ppm].

An Optizen UV-Vis 9582 spectrophotometer was used to measure the BSA concentration at a wavelength of 280 nm.

Figure 1 – Experimental set-up for ultrafiltration test

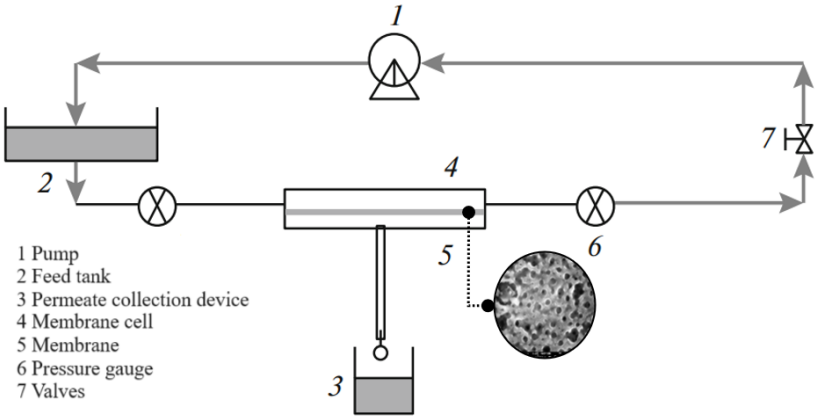

Source: Authors.

3 RESULTS AND DISCUSSIONS

3.1 MORPHOLOGY

The PET bottle shards and granulated PEG demonstrated complete solubility in the TCA: DCM solvent, forming clear polymer solutions upon blending. Afterward, these solutions were poured onto a glass plate and submerged in a distilled water bath to solidify, forming membranes. Figure 2 visually represents PET membranes prepared using varying proportions of PEG, depicting flawlessly smooth surfaces devoid of defects. However, an elevation in PEG concentration beyond 30% led to flaws in the form of holes visible to the naked eye. Furthermore, the study observed distinct mechanical properties among the membranes: M1 displayed stiffness, while M2, M3, and M4 exhibited increased flexibility, a common trait associated with PEG as a plasticizing agent known to enhance polymer film flexibility (CIARAMITARO et al., 2023; ESLAMI et al., 2023; OH et al., 2014). Despite the standardized 100 µm thickness of the cast solution for the prepared membranes, post-coagulation, M1 retained its original thickness, whereas M2, M3, and M4 exhibited reduced thicknesses of 84 µm, 75 µm, and 59 µm, respectively. This reduction in thickness in M2, M3, and M4 after coagulation is attributed to the heightened solubility of polyethylene glycol (PEG) in the water coagulation bath. The consistent decrease in membrane thickness aligned with the escalating proportion of PEG, as demonstrated in Figure 3, indicating a clear inverse relationship between PEG concentration and resulting membrane thickness.

Figure 2 – Photographs of the surfaces of the PET membranes prepared using varying molecular weights of PEG

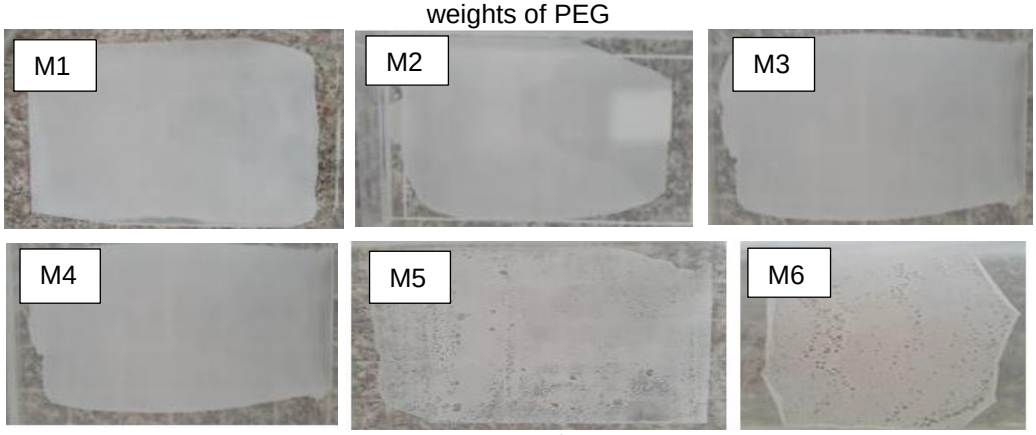

Source: Authors.

Figure 3 – Effect of different PEG % on the average thickness of the membranes

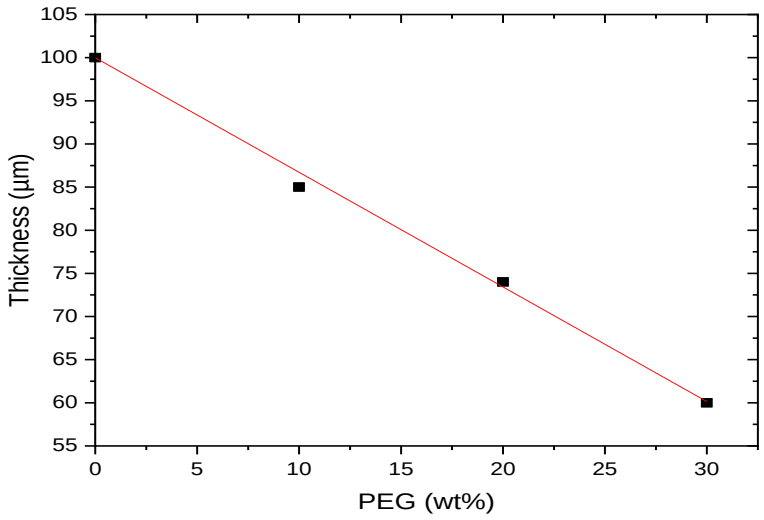

Source: Authors.

Moreover, the assessment of membrane hydrophilicity involved measuring the water contact angle, with results detailed in Table 2. Incorporating PEG into the PET membrane enhanced its hydrophilic properties, as evidenced by a decreased water contact angle. Enhancing hydrophilic properties is essential in advancing ultrafiltration membranes employed in water treatment. Previous studies reported increased hydrophilicity in other polymer membranes like PVDF(GAYATRI et al., 2023), PS (AKTAS EKEN; ACAR, 2020), and PES (PURUSHOTHAMAN et al., 2023) upon adding PEG.

Table 2 – The presence of the casting solutions and the subsequent membranes containing various additives

Membrane	PEG (wt%)	Water contact angle (°)
M1	No additive	65.5
M2	10	61.9
M3	20	60.3
M4	30	59.7

Source: Authors.

3.2 SURFACE CHARACTERIZATION

SEM pictures in Figure 4 illustrate the surface and cross-sectional views of PET membranes obtained from PET bottles with different PEG concentrations. The structure found in all membranes is characterized by asymmetry, consisting of a supportive layer with a large-pored cross-section and a thin, sleek layer that functions as the active surface of the membrane. Macro-voids may be observed in M3 and M4, indicating a change in shape caused by a delayed separation process during membrane formation. The delayed separation of components causes the construction of a porous morphology, while immediate separation usually leads to the development of a finger-shaped structure inside the membrane (PURKAIT et al., 2018). The cross-sectional scanning electron microscopy (SEM) analysis of pure polyethylene terephthalate (PET) membrane M1 (Figure 4-b) shows a composite membrane structure. It consists of two layers, one layer with a non-porous area and the other layer considered as a support sub-layer with an existing porous area. The Surface study of M1 (Figure 4-a) reveals a low number of aggregate voids, which is believed to be the primary path connecting the isolated porous layer. Modifying the concentration of PEG in the casting solution causes modifications in the membrane structure, remarkably increasing the creation of pores when immersed in the nonsolvent. When 10% PEG was added to the M2 membrane, it resulted in a uniform and porous sublayer with more precise holes than the M1 membrane. Adding more than 10% causes macro-voids to form, indicating increased porosity regions. The study keeps the PEG molecular weight (Mn-6000), coagulation bath temperature (25 ºC), and evaporation duration (5 min) the same before immersion. It attributes the presence of macro-voids in M3 and M4 mainly to the high PEG content above 10%.

Figure 5 illustrates the surface characteristics of the PET membranes, encompassing hole distribution and dimensions. These images were analyzed using ImageJ, employing the threshold value technique to derive binary images

from scanning electron microscopy (SEM) images, following established methodologies (HOJAT et al., 2023; ZHANG et al., 2015). SEM analysis of the membrane surfaces (Figure 4) distinctly demonstrates alterations in the sublayer surface morphology, notably marked by the formation of macrovoids whose diameters conspicuously increase with higher PEG content. This trend is particularly evident in M3 and M4, with M4 displaying substantially larger voids than M3, and adding 10% more PEG in M4 than in M3 results in a tripling of macrovoid diameter from 35 µm to 100 µm. Upon detailed scrutiny of the top surfaces (Figure 5-A), pure PET membrane M1 exhibits negligible pore formation on the sublayer surface, with a rare occurrence of singular pores. Conversely, M2 displays a more uniform and smoother surface, markedly augmented by the addition of PEG, resulting in a significantly porous surface featuring pores ranging from approximately 0.05 µm to 5 µm, predominantly in the 0.05-1 µm range. The higher PEG concentration in membrane M3 leads to a profusion of voids, with pores evident on both the surface and extensively within macrovoid structures (Figure 5-B). The pore size distribution ranges from 0.29 µm to 7.47 µm, with the majority varying from 0.29 µm to 29.8 µm. SEM imaging of M4 highlights membrane structures within macrovoids exceeding 100 µm in diameter, revealing internal pores exclusively within macrovoids. Consequently, the surface analysis focuses on these internal pores, ranging from 0.7 µm to 9.46 µm, with a predominant size range of 0.7 µm to 29.8 µm. The average pore diameter on the sublayer surface exhibits an ascending trend correlated with higher PEG ratios, attributed to the macrovoid structure contributing to an enlargement in pore size. This trend aligns with findings from prior research involving PEG as an additive in polysulfone membranes (YUNOS et al., 2014).

Figure 4 – Image analysis using scanning electron microscopy of PET membranes made from PET bottles with varying amounts of PEG, showing (a) the top surface and (b) a cross-section

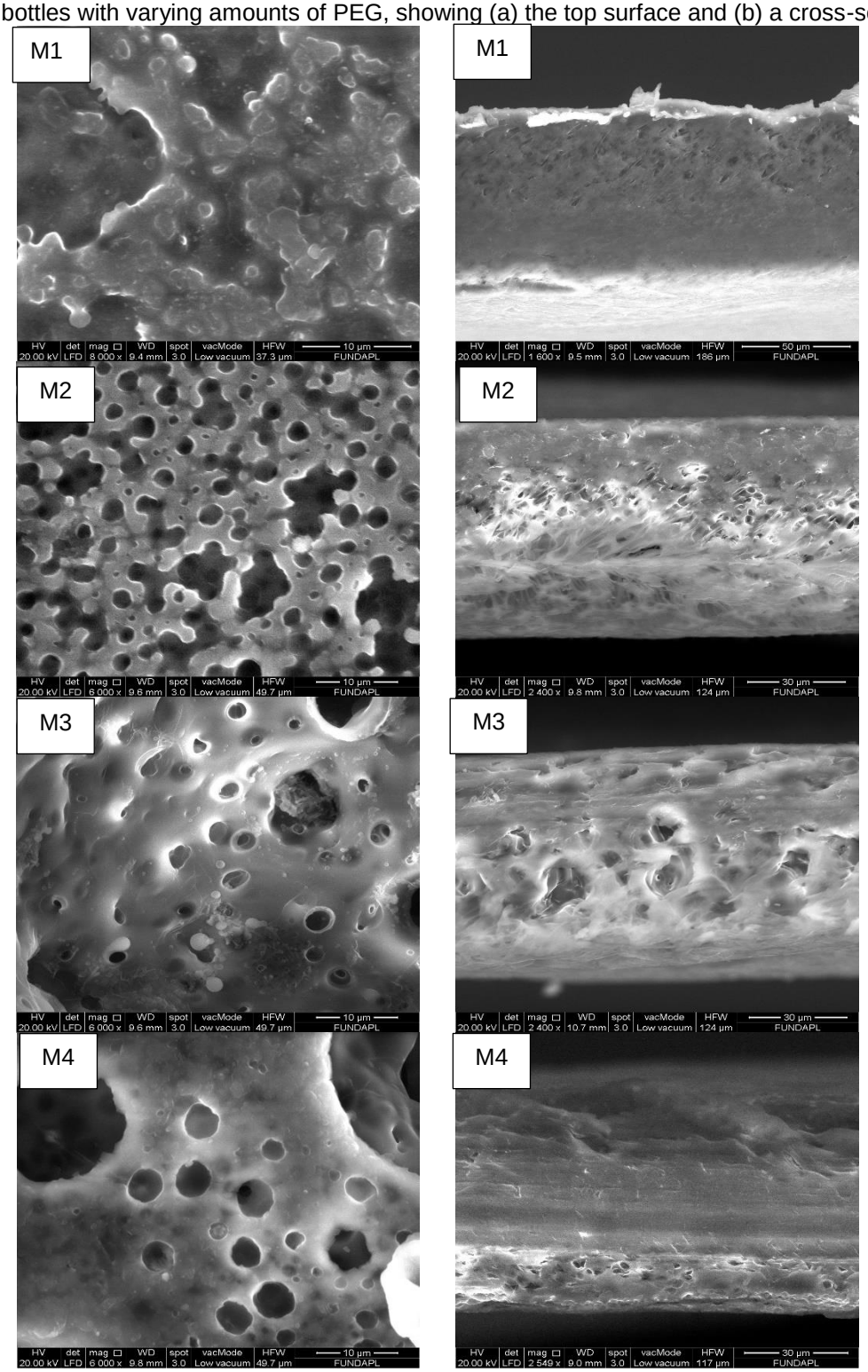

(a) Top surface (b) Cross-sections

Source: Authors.

Figure 5 – Analysis of SEM images of a membrane surface determines (a) The distribution of pore sizes within the membranes and (b) The identification of pores in binary SEM images, where pores are denoted in black and the membrane matrix in white

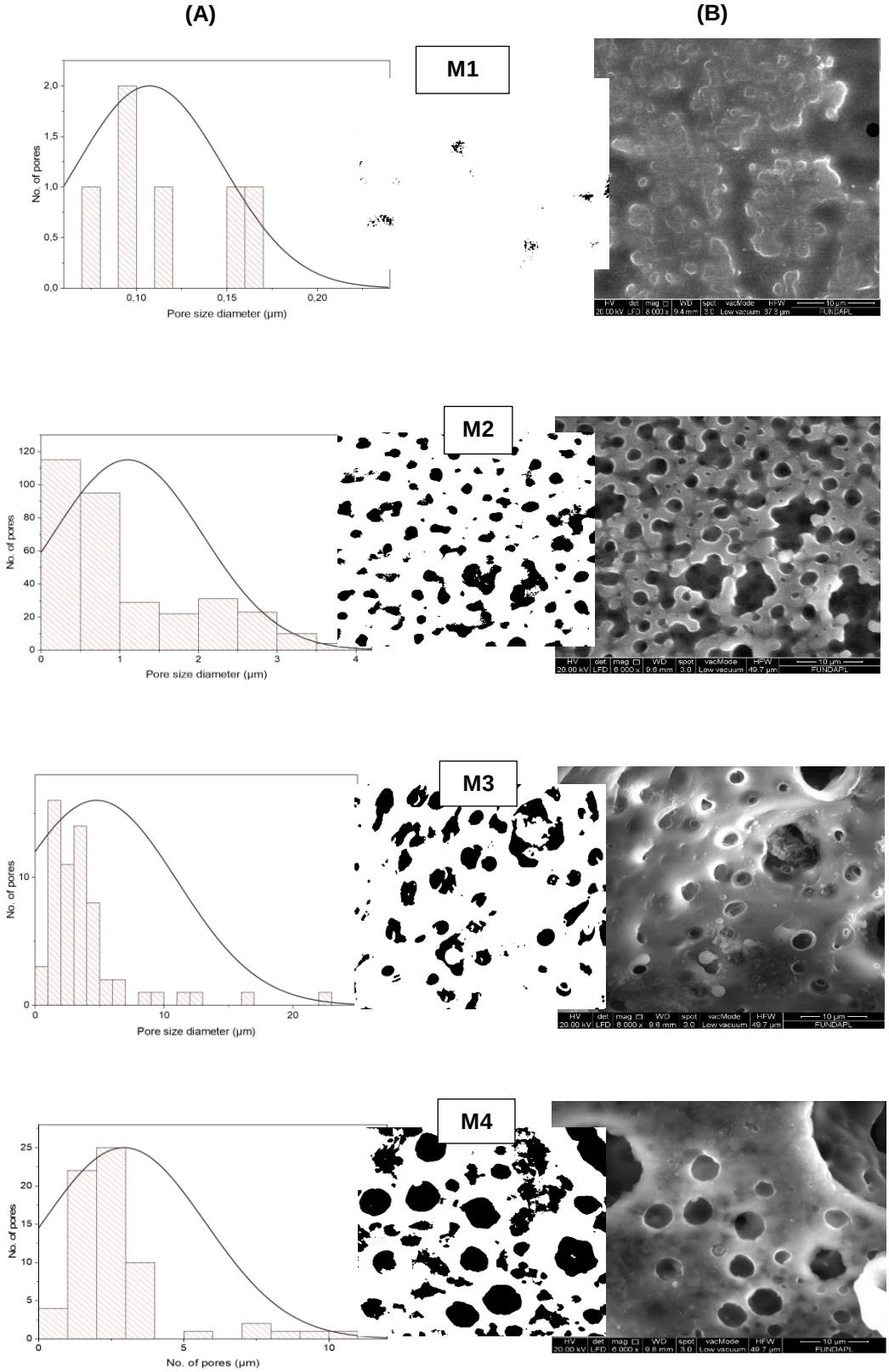

Source: Authors.

Contrary to expectations, EDS analysis reveals chlorine atoms in fabricated membranes (M1, M2, M3, M4), primarily from a dichloromethane and trichloroacetic acid solvent mixture. Notably, the constituents used in membrane preparation, namely PET polymer Poly (ethylene terephthalate) and PEG Poly (ethylene glycol) possessing general formulas H-(O−CH_2−CH_2)n−OH and (−OOC−C_6H_5−COOCH_2−CH_2−)n, primarily comprise carbon (C), oxygen (O), and hydrogen (H), as revealed in Figure 6.

Figure 6 – EDS images illustrating the surface of PET membranes

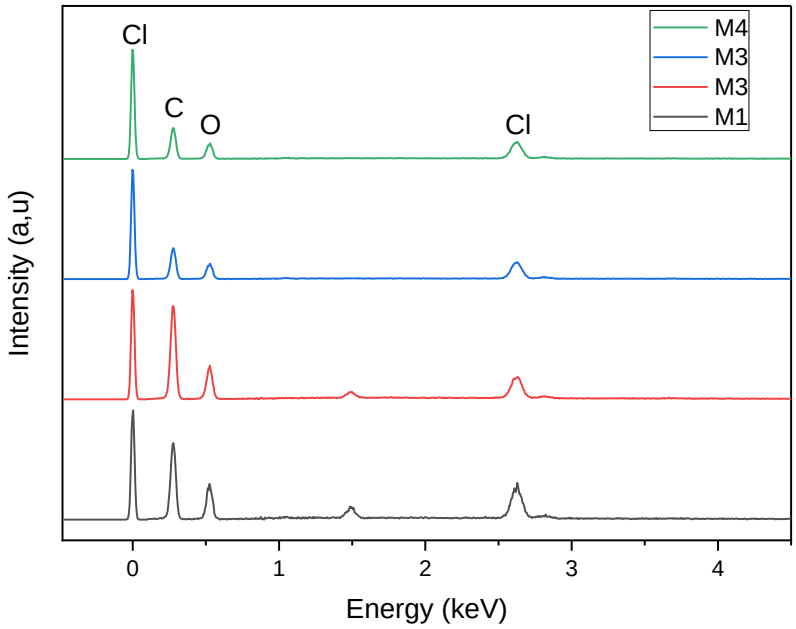

Source: Authors.

3.3 WATER VAPOR PERMEABILITY

Figure 7 illustrates the impact of the PEG ratio in casting solution on water vapor permeability (WVP), demonstrating its substantial influence. The PET membrane, devoid of additives M1, displayed a significant 316 x 10+2 barrer permeability. Membrane M2 exhibited a WVP of 534 x 10^{+2} barrer, whereas M3 and M4 recorded WVP values of 1068 x 10^{+2} barrer and 1110 x 10^{+2} barrer, respectively. Including PEG in the membrane casting solution led to membranes with enhanced water permeability. Including PEG additives in the casting solution impacted the size of the pores in the membrane. A conceptual association exists

between ultrafiltration membrane permeability and pore size (KANANI et al., 2010; SIDDIQUI; ARIF; BASHMAL, 2016).

Figure 7 – Permeability of water vapor in the prepared membranes

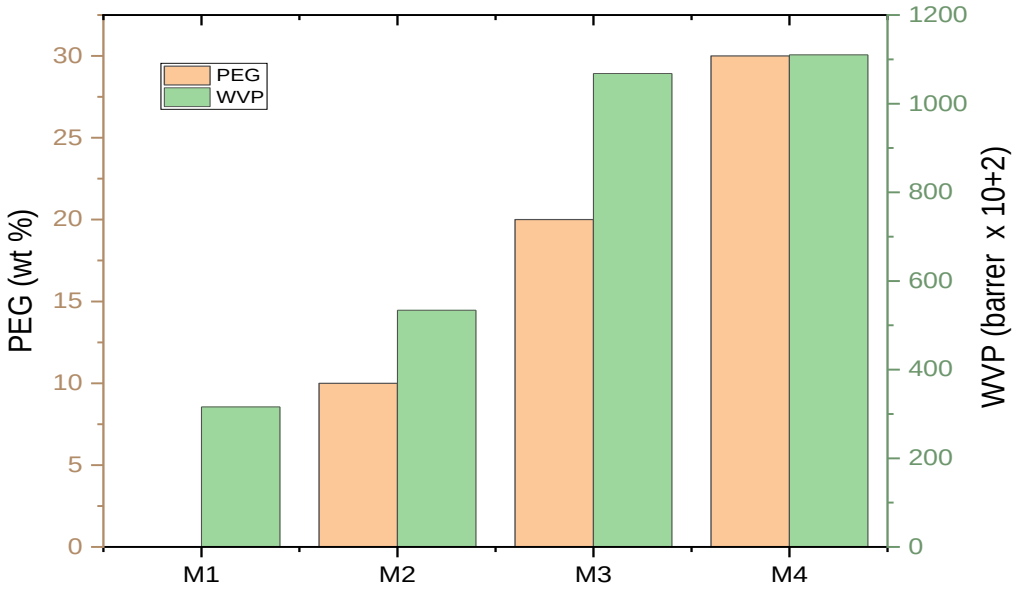

Source: Authors.

3.4 ULTRAFILTRATION MEMBRANES

Ultrafiltration experiments conducted using membranes M2, M3, and M4 proceeded without any observed flaws. The PET membrane lacking additives was not utilized in the ultrafiltration experiments due to its limited flexibility, rendering it incompatible with the membrane module. Figure 8 presents the BSA rejection values obtained. Initially, membrane M2 exhibited a rejection rate of 95.30%, gradually decreasing to 79% during the treatment period, achieving an elimination rate of 88.4% over 120 minutes. In contrast, membrane M3 showcased maximum rejection rates of 66% within the initial 20-minute treatment interval, stabilizing at 5%. The rejection pattern for M4 started at 49% and decreased to 2% due to the macrovoid porous nature it embodies. Notably, M2 exhibited a higher BSA molecule rejection rate of 95.3% compared to M3 and M4, aligning with the SEM analysis results depicting smaller pores in the M2 membrane. Consequently, despite a substantial decline in flux compared to M3 and M4, M2 demonstrated the most marked improvement in anti-fouling properties.

Figure 8 – BSA rejection by PET membranes with various contents of PEG

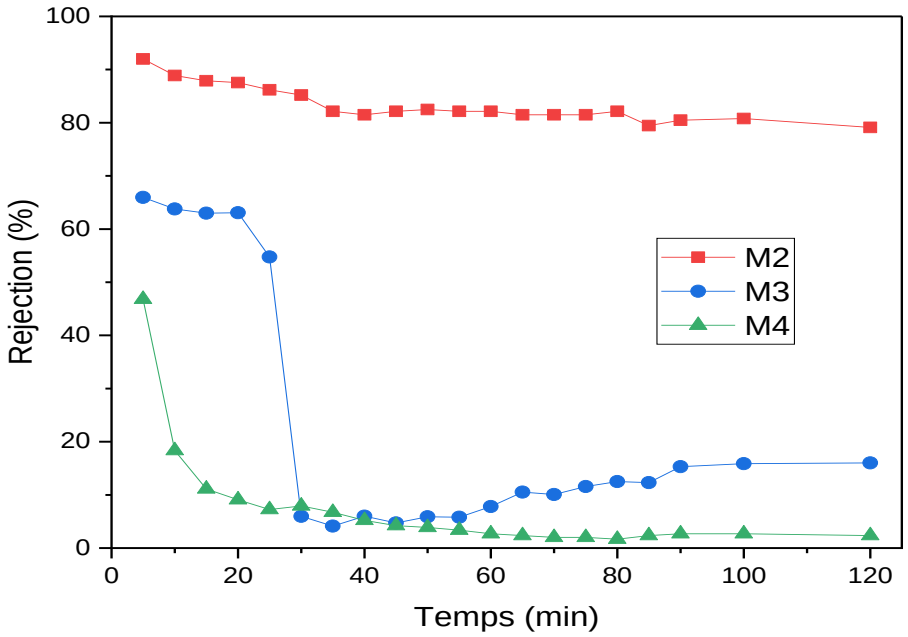

Source: Authors.

4 CONCLUSION

This study extensively explores synthesizing and evaluating ultrafiltration membranes crafted from recycled PET waste. The investigation showcases the successful fabrication of asymmetric PET-based membranes blended with PEG, highlighting the nuanced impact of PEG ratios on membrane morphology, surface characteristics, and permeability. The observed increase in pore size with higher PEG content aligns with the membranes' augmented water vapor permeability, demonstrating the pivotal role of PEG in enhancing membrane properties. EDS analysis unexpectedly detects chlorine atoms in the membranes, attributed to the solvent mixture utilized in fabrication. Furthermore, ultrafiltration experiments underscore the significance of PEG-induced alterations, with membrane M2 displaying superior anti-fouling attributes despite reduced flux. This study highlights the feasibility of repurposing PET waste into functional membranes while emphasizing the need for optimization strategies to refine membrane performance for diverse applications in separation technologies.

ACKNOWLEDGMENT

The present work is supported by Algeria's DGRSDT (General Directorate of Scientific Research and Technological Development).

REFERENCES

AKTAS EKEN, G.; ACAR, M. H. Polysulfone-based amphiphilic copolymers: Effect of hydrophilic content on morphology and performance of ultrafiltration membranes. **Journal of Applied Polymer Science**, v. 137, n. 4, p. 48306, 20 jan. 2020. https://doi.org/10.1002/APP.48306

BEGHETTO, V. et al. Recent Advancements in Plastic Packaging Recycling: A Mini-Review. **Materials 2021, Vol. 14, Page 4782**, v. 14, n. 17, p. 4782, 24 ago. 2021. https://doi.org/10.3390/MA14174782

C16.33 COMMITTEE. **Standard Test Methods for Water Vapor Transmission of Materials**. USA04.06, 2013. Disponível em: <https://www.astm.org/e0096_e0096m-10.html>. Acesso em: 31 dez. 2023 https://doi.org/10.1520/E0096_E0096M-10

CIARAMITARO, V. et al. From micro to macro: Physical-chemical characterization of wheat starch-based films modified with PEG200, sodium citrate, or citric acid. **International Journal of Biological Macromolecules**, v. 253, p. 127225, 31 dez. 2023. https://doi.org/10.1016/J.IJBIOMAC.2023.127225

ESLAMI, Z. et al. A Review of the Effect of Plasticizers on the Physical and Mechanical Properties of Alginate-Based Films. **Molecules 2023, Vol. 28, Page 6637**, v. 28, n. 18, p. 6637, 15 set. 2023. https://doi.org/10.3390/MOLECULES28186637

GAYATRI, R. et al. Preparation and Characterization of PVDF–TiO2 Mixed-Matrix Membrane with PVP and PEG as Pore-Forming Agents for BSA Rejection. **Nanomaterials 2023, Vol. 13, Page 1023**, v. 13, n. 6, p. 1023, 2023. https://www.mdpi.com/2079-4991/13/6/1023

GEBRU, K. A.; DAS, C. Effects of solubility parameter differences among PEG, PVP and CA on the preparation of ultrafiltration membranes: Impacts of solvents and additives on morphology, permeability and fouling performances. **Chinese Journal of Chemical Engineering**, v. 25, n. 7, p. 911–923, 1 jul. 2017. https://doi.org/10.1016/J.CJCHE.2016.11.017

HAFANI, M. et al. Formulation and characterization of a new PET-based membrane for methane gas dehydration. **Polymer-Plastics Technology and Materials**, v. 60, n. 15, p. 1605–1619, 13 out. 2021. https://doi.org/10.1080/25740881.2021.1912091

HOJAT, N. et al. Automatic pore size measurements from scanning electron microscopy images of porous scaffolds. **Journal of Porous Materials**, v. 30, n. 1, p. 93–101, 1 fev. 2023. https://doi.org/10.1007/S10934-022-01309-Y/FIGURES/10

JAREONSRI, L.; NAWALERTPANYA, S.; JANTAPORN, W. Preparation and Characterization of Novel Membrane from Waste Polyethylene terephthalate and Bio-based Polymer. **IOP Conference Series: Materials Science and**

Engineering, v. 1280, n. 1, p. 012010, 1 abr. 2023. *Materials Science and Engineering*, *1280*(1), 012010. https://doi.org/10.1088/1757-899X/1280/1/012010

KANANI, D. M. et al. Permeability–selectivity analysis for ultrafiltration: Effect of pore geometry. **Journal of Membrane Science**, v. 349, n. 1–2, p. 405–410, 1 mar. 2010. https://doi.org/10.1016/J.MEMSCI.2009.12.003

KIBRIA, M. G. et al. Plastic Waste: Challenges and Opportunities to Mitigate Pollution and Effective Management. **International Journal of Environmental Research**, v. 17, n. 1, p. 1–37, 1 fev. 2023. https://doi.org/10.1007/S41742-023-00507-Z/FIGURES/26

KIRSHANOV, K. et al. Recent Developments and Perspectives of Recycled Poly(ethylene terephthalate)-Based Membranes: A Review. **Membranes 2022, Vol. 12, Page 1105**, v. 12, n. 11, p. 1105, 5 nov. 2022. https://doi.org/10.3390/MEMBRANES12111105

LIN, C. Y. et al. Smart temperature-controlled water vapor permeable polyurethane film. **Journal of Membrane Science**, v. 299, n. 1–2, p. 91–96, 1 ago. 2007. https://doi.org/10.1016/J.MEMSCI.2007.04.028

MA, Y. et al. Preparation and characterization of PSf/clay nanocomposite membranes with PEG 400 as a pore forming additive. **Desalination**, v. 286, p. 131–137, 1 fev. 2012. https://doi.org/10.1016/J.DESAL.2011.10.040

MULYATI, S. et al. Fabrication of hydrophilic and strong pet-based membrane from wasted plastic bottle. **Rasayan Journal of Chemistry**, v. 11, n. 4, p. 1609–1617, 1 out. 2018. https://doi.org/10.31788/RJC.2018.1144047

OH, H. J. et al. Rheological studies of disulfonated poly(arylene ether sulfone) plasticized with poly(ethylene glycol) for membrane formation. **Polymer**, v. 55, n. 6, p. 1574–1582, 24 mar. 2014. https://doi.org/10.1016/J.POLYMER.2014.02.011

PULIDO, B. A. et al. Recycled Poly(ethylene terephthalate) for High Temperature Solvent Resistant Membranes. **ACS Applied Polymer Materials**, v. 1, n. 9, p. 2379–2387, 22 jul. 2019. https://doi.org/10.1021/ACSAPM.9B00493

PURKAIT, M. K. et al. Introduction to Membranes. **Interface Science and Technology**, v. 25, p. 1–37, 1 jan. 2018. https://doi.org/10.1016/B978-0-12-813961-5.00001-2

PURUSHOTHAMAN, M. et al. Enhancement of antifouling properties, metal ions and protein separation of poly(ether-ether-sulfone) ultrafiltration membranes by incorporation of poly ethylene glycol and n-ZnO. **Environmental Research**, v. 216, p. 114696, 1 jan. 2023. https://doi.org/10.1016/J.ENVRES.2022.114696

RAJ, B. et al. Advancements in PET Packaging: Driving Sustainable Solutions for Today's Consumer Demands. **Sustainability 2023, Vol. 15, Page 12269**, v. 15, n. 16, p. 12269, 11 ago. 2023. https://doi.org/10.3390/SU151612269

RAJESH, S.; MURTHY, Z. V. P. Ultrafiltration membranes from waste polyethylene terephthalate and additives: synthesis and characterization. **Química Nova**, v. 37, n. 4, p. 653–657, 2014. https://doi.org/10.5935/0100-4042.20140097

SIDDIQUI, M. U.; ARIF, A. F. M.; BASHMAL, S. Permeability-Selectivity Analysis of Microfiltration and Ultrafiltration Membranes: Effect of Pore Size and Shape Distribution and Membrane Stretching. **Membranes 2016, Vol. 6, Page 40**, v. 6, n. 3, p. 40, 6 ago. 2016. https://doi.org/10.3390/MEMBRANES6030040

YUNOS, M. Z. et al. Studies on fouling by natural organic matter (NOM) on polysulfone membranes: Effect of polyethylene glycol (PEG). **Desalination**, v. 333, n. 1, p. 36–44, 15 jan. 2014. https://doi.org/10.1016/J.DESAL.2013.11.019

ZHANG, Y. et al. Characterization of the pore size distribution with SEM images processing for the tight rock. **2015 IEEE International Conference on Information and Automation, ICIA 2015 – In conjunction with 2015 IEEE International Conference on Automation and Logistics**, p. 653–656, 28 set. 2015. https://doi.org/10.1109/ICINFA.2015.7279367